Study of Spin-Polarized Transport Properties for Spin-FET Design Optimization

Semion Saikin, Min Shen, and Ming-C. Cheng, *Member, IEEE*

***Abstract*—A Monte Carlo method developed previously for spin dynamics is applied to study spin-polarized transport properties of two–dimensional electron gas in semiconductor spin-FET structure. The specific symmetry of spin-orbit terms (Rashba and Dresselhaus) leads to strong anisotropy of spin dynamics in the low field regime. Coherent spin evolution and spin dephasing are investigated for different orientations of the device channel related to the crystallographic axes. Efforts have been made to suppress spin dephasing while conserving coherent oscillation of spin polarization required for spin-FET design. Results derived from this study provide useful information to assist in optimization of the spin-FET performance.**

***Index Terms*—Anisotropy, Monte Carlo, spin relaxation, spintronics, spin-FET.**

I. Introduction

UTILIZATION of spin-dependent phenomena in electronic devices is one of the promising approaches for future electronics [1]–[3]. While some magnetoelectronic devices, exploiting the tunneling magnetoresistance and giant magnetoresistance effects in ferromagnetic-layer structures, have been developed and used in modern industry, more universal and more promising semiconductor spin-FETs [4]–[6] or bipolar spin-transistors [7]–[9] are at an early stage of progress. The key property of magnetoelectronics or spintronics is that the electron spin can be used to encode information in the spin-polarized current. Specific device design and selection of material properties may be needed to effectively utilize the current spin polarization. Some of these features may actually lead to undesirable effects. For example, the strong spin-orbit coupling, which is required for the spin-FET proposed by Datta and Das [4], in the presence of electron momentum scatterings, produces the fast D'yakonov–Perel spin relaxation [10]. Even more pronounced spin dephasing can occur due to effect of magnetic contacts [11].

Manuscript received August 10, 2003; revised Ocotber 17, 2003. This research was supported in part by the National Security Agency and Advanced Research and Development Activity under Army Research Office Contract DAAD-19-02-1-0035, and in part by the National Science Foundation under Grant DMR-0121146.

S. Saikin is with the Center for Quantum Device Technology and Department of Electrical and Computer Engineering, Clarkson University, Potsdam, NY 13699 USA, and also with the Physics Department, Kazan State University, Kazan 420008, Russia (e-mail: saikin@clarkson.edu).

M. Shen and M. C. Cheng are with the Center for Quantum Device Technology and Department of Electrical and Computer Engineering, Clarkson University, Potsdam, NY 13699 USA (e-mail: shenm@clarkson.edu; mcheng@clarkson.edu).

Digital Object Identifier 10.1109/TNANO.2004.824021

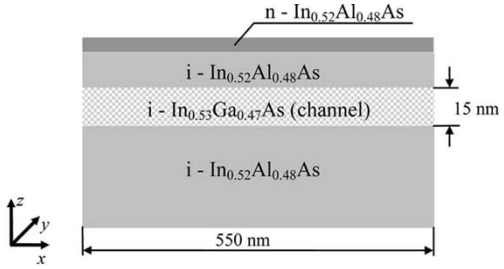

Fig. 1. Device structure for the simulations.

Transport parameters for spintronic devices are still not well studied. In order to understand the spin-dependent transport phenomena, realistic models accounting for spin-dependent scattering and interaction are needed. The Monte Carlo approach, which is able to incorporate evolution of the electron spin polarization [12]–[16] and provide physical insight into the spin dynamics, is one of the possible tools for study of the spin-dependent transport properties. This approach goes beyond the approximations of the drift-diffusion and hydrodynamic transport models, and can easily accommodate distinctive device features [17], [18].

In this work, we study properties of spin-polarized current in an $In_{0.52}Al_{0.48}As/In_{0.53}Ga_{0.47}As$ FET structure shown in Fig. 1, using a Monte Carlo method developed in a previous study [14]. Similar structures have been proposed for designing spin-FETs [4]–[6]. We focus on the case with the spin injection in the configuration of the spin-FET proposed by Datta and Das [4]. At the source contact, spin polarization is assumed to be parallel with the current direction, and the polarization coherently evolves along the channel. Of particular interest in our work is the anisotropy of spin dynamics related to the transport direction [19], [6]. Based on the analysis of spin-orbit interaction influenced by the transport direction related to the crystallographic axes, we optimize the device channel orientation to improve performance of the spin-FET.

The paper is organized as follows. In Section II, we review the theoretical model applied to simulations. The anisotropic spin scattering matrix accounting for spin-orbit interaction is derived. In Section III, this model is applied to simulation of spin-polarized transport of electrons in the single quantum well (QW) of the FET structure shown in Fig. 1. Different orientations of the device channel related to the crystallographic axes are considered. We search for regime with a long spin dephasing length applicable to spin-FETs. In Section IV, physics of simulated results is discussed. The paper is concluded in Section V.

II. Theory

We select the heterostructure layers of the spin-FET, given in Fig. 1, orthogonal to the (0, 0, 1) direction in the crystallographic axes. The device coordinate system is defined as follow. The z axis of the device coordinate system is parallel to the (0, 0, 1) crystallographic direction, and the x axis is oriented along the device channel. It forms an angle ξ with the (1, 0, 0) crystallographic direction in the plane of the two-dimensional (2-D) electron gas.

In the simulation, thermalized electrons, injected at the left boundary, travel along the channel due to the applied drain–source voltage, $V_{\rm DS}$, and are absorbed at the right boundary. For the spatial electron evolution, we assume that the z component of the electron momentum is quantized, while the motion in the xy plane is classical. This is an appropriate approximation for submicrometer or deep-submicrometer devices with a smooth potential along the channel at room temperature. For electron scatterings, ionized impurity, acoustic-phonon, and optical-phonon scattering mechanisms are considered. The electric field along the channel is calculated from the Poisson equation self-consistently with the electron motion and updated at each time step. During the "free flight" time, δt, which is the smaller of the time step and the time interval between two scattering events, the electrons propagate with a constant acceleration. The details of the Monte Carlo method for spin-polarized transport are presented elsewhere [15].

For the description of an electron spin dynamics, we use the spin density matrix [20]

$$\boldsymbol{\rho} = \begin{pmatrix} \rho_{\uparrow\uparrow} & \rho_{\uparrow\downarrow} \\ \rho_{\downarrow\uparrow} & \rho_{\downarrow\downarrow} \end{pmatrix}. \tag{1}$$

This representation is defined using the spin expectation values for a single quantum particle or applying an additional classical average over a system of quantum particles. The physical meaning for the diagonal element, $\rho_{\uparrow\uparrow,\downarrow\downarrow}$, is the probability to find the spin in the "up" or "down" state (parallel or antiparallel to the z axis). The complex conjugate off-diagonal element, $\rho_{\uparrow\downarrow,\uparrow\downarrow}$, describes the coupling between the "up" and "down" states in a given coordinate system. The mathematical formalism for the evolution of the spin density matrix is well developed and widely used in the optical [20] and magnetic resonance [21] spectroscopy.

While the spin density matrix is useful for the modeling of spin dynamics, the spin polarization vector $\mathbf{P}$ is more convenient for pictorial presentation. It is closely related with the definition of the density matrix

$$\begin{aligned} \rho_{\uparrow\uparrow,\downarrow\downarrow} &= (1 \pm P_z)/2 \\ \rho_{\uparrow\downarrow,\uparrow\downarrow} &= (P_x \mp iP_y)/2. \end{aligned} \tag{2}$$

To calculate the current spin polarization at position $\mathbf{r}$, we average the density matrices for all electrons in a small volume d^3r near $\mathbf{r}$ with the inplane wave number in a momentum area d^2k near $\mathbf{k}$. This description is possible because the spatial motion is treated classically with momentum $\hbar\mathbf{k}$. The averaged spin density matrix, $\langle\rho(\mathbf{r},\mathbf{k},t)\rangle$, is then an analog of the distribution function for spin-polarized electrons. The average spin density matrix can be projected onto the Pauli matrix space using $f_\alpha = \mathrm{Tr}(\sigma_\alpha\langle\rho\rangle)$, together with the diagonal unity matrix I, where σ_α is the set of the three Pauli matrices, $\alpha = x, y, z$, and I corresponds to the nonpolarized state ($\alpha = n$). Similarly to the quantities defined as moments of the nonpolarized electron distribution function, f_n, one can obtain the spin density $n_\alpha(\mathbf{r},t)$ and spin current density components $j_\alpha(\mathbf{r},t)$, etc., as moments of the distribution functions f_x, f_y or f_z. In this work, we present only the steady state results for the set of the zeroth-order moments normalized by the local electron density, $P_\alpha(\mathbf{r}) = n_\alpha(\mathbf{r})/n_n(\mathbf{r})$, which yield the components of the spin polarization vector. The spin-polarization vector $\mathbf{P}(\mathbf{r})$ satisfies $|\mathbf{P}(\mathbf{r})| \leq 1$. It is equal to 1 for completely spin-polarized current, and 0 for nonpolarized current.

In general, the evolution of electron spin in semiconductor heterostructure is influenced by many different factors: external and local magnetic fields, spin-orbital interaction, and electron-electron interaction, etc. In this work, we assume that the electron spin dynamics is only determined by the interaction of the spin with the electron momentum due to the spin-orbit term $H_{\rm SO}(\mathbf{k})$. This conventional assumption is a basis for the Datta and Das Spin-FET [4]. Traditionally, two different terms of the spin-orbit interaction [22], [23] are considered for an asymmetric single QW structure (Fig. 1). The origin of the Dresselhaus term [22] is the bulk inversion asymmetry of the crystal, while the Rashba term [23] is produced by the structure inversion asymmetry of the QW. For a relatively narrow QW, these terms are linear functions of electron momentum. While the Rashba spin-orbit term

$$H_{\rm R} = \eta(k_y\sigma_x - k_x\sigma_y) \tag{3}$$

is independent of the device channel orientation related to the crystallographic axes, the Dresselhaus term

$$\begin{aligned} H_{\rm D} = \beta\left\langle k_z^2\right\rangle &((k_y\sigma_y - k_x\sigma_x)\cos 2\xi \\ &+ (k_y\sigma_x + k_x\sigma_y)\sin 2\xi) \end{aligned} \tag{4}$$

is determined by the angle, ξ, between the device channel (x axis) and the (1, 0, 0) crystallographic direction. The spin-orbit coupling constants η and β are dependent on the material band structure and the shape of the confining potential [24], [25].

During the "free flight," δt, the single electron density matrix evolves as

$$\boldsymbol{\rho}(t+\delta t) = \mathbf{S}(\mathbf{k},\delta t)\boldsymbol{\rho}(t)\mathbf{S}^{-1}(\mathbf{k},\delta t). \tag{5}$$

In simulations, if δt is small enough, the momentum $\mathbf{k}$ in (5) is taken as the average electron momentum during its "free flight." The spin scattering matrix $\mathbf{S}(\mathbf{k},\delta t)$ can be written as

$$\mathbf{S}(\mathbf{k},\delta t) = \begin{pmatrix} \cos(|\alpha|\delta t) & i\frac{\alpha}{|\alpha|}\sin(|\alpha|\delta t) \\ i\frac{\alpha^*}{|\alpha|}\sin(|\alpha|\delta t) & \cos(|\alpha|\delta t) \end{pmatrix} \tag{6}$$

where the parameter, α, is determined by the interaction described in (3) and (4). Using the spin-orbit coupling constants, it can be shown that

$$\begin{aligned} \alpha = \hbar^{-1}\{&\left(k_y\left(\eta + \beta\left\langle k_z^2\right\rangle\sin 2\xi\right) - k_x\beta\left\langle k_z^2\right\rangle\cos 2\xi\right) \\ &- i\left(k_x\left(\beta\left\langle k_z^2\right\rangle\sin 2\xi - \eta\right) + k_y\beta\left\langle k_z^2\right\rangle\cos 2\xi\right)\}. \end{aligned} \tag{7}$$

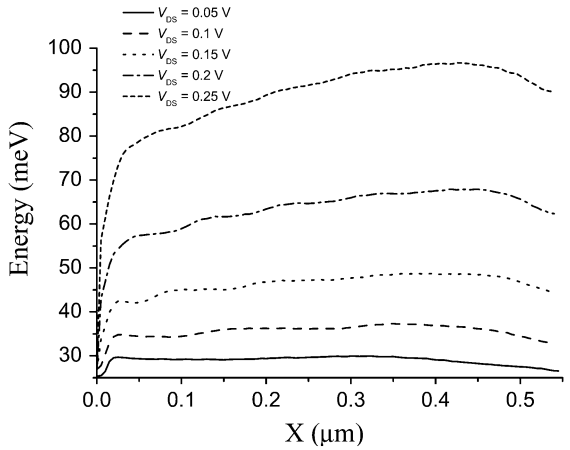

Fig. 2. Energy profiles for $T = 300$ K.

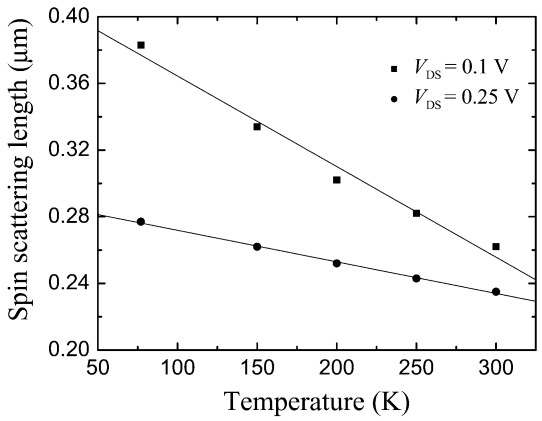

Fig. 3. Spin scattering length as a function of temperature. The device channel is oriented parallel to the (1, 0, 0) crystallographic direction. Injected spin polarization is in the channel direction.

Each momentum scattering event changes the spin-orbit interaction and influences the subsequent electron spin evolution. For a system of electrons possessing the same spin orientation, the spatial electron motion with the evolution operator in (5) can result in coherent rotation of the spin polarization as well as spin dephasing (loss of spin polarization). The angular dependence of the spin scattering matrix in (6) should be reflected in both processes.

III. Simulation

The length of the considered device is $L_{\rm D} = 550$ nm, and the width is infinite. The confining potential is an asymmetric single QW (width $d = 15$ nm) in the z direction. We assume that the equilibrium 2-D electron density in the device channel is $N_S = 0.9 \times 10^{12}$ cm^{-2}. The conduction band parameters for $In_{0.53}Ga_{0.47}As$ were taken from [26]. The spin-orbit coupling constants are crucial parameters for simulation of the spin polarization. Experimental values vary widely. We estimate the Rashba spin-orbit coupling constant with the $In_{0.53}Ga_{0.47}As$ band parameters [26] according to the formula from [24] ($\eta = 0.576 \cdot 10^{-9}$ eVcm). The Dresselhaus constant is interpolated from the parameters for GaAs [25] and InAs [27] ($\beta = 0.644 \cdot 10^{-22}$ eVcm^3). The average value of the electric field in the z direction used for calculation of Rashba coupling constant and $\langle k_z^2 \rangle$ is $\langle E_z \rangle = 240$ kV/cm. $\langle E_z \rangle$ is assumed to be constant along the device channel. The applied drain–source voltage, $V_{\rm DS}$, ranges from 0.05 to 0.25 V. The upper limit of the voltage is selected to reduce population of excited subbands in the QW, which allows us to use the one subband approximation [14].

The calculated average energy profiles in the device channel for different values of $V_{\rm DS}$ are shown in Fig. 2. Because, in the structure for the simulation, there is no high doping concentration near $x = 0$ to maintain low electric field, the field increases rapidly near the source boundary, and the transport is nearly ballistic. Within the small ballistic distance from the injection boundary, $l \approx 0.02$ μm (depending on the applied voltage), electrons gain enough energy such that the optical phonon emission scattering becomes dominant. Electrons are then gradually thermalized. Due to low applied voltage, the transport in the rest of device is almost drift-diffusive.

The injected electrons at $x = 0$ are assumed completely spin polarized. The macroscopic parameter, spin dephasing or spin scattering length, $L_{\rm SS}$, is usually used to characterize loss of spin polarization. We define it as the length where current spin polarization is reduced to $1/e$ of the injected value. For different spin-FET designs, different device length related to $L_{\rm SS}$ may be needed. The spin-FET proposed by Datta and Das [4] functions with $L_{\rm D} \approx L_{360} \ll L_{\rm SS}$, where L_{360} is the characteristic length for the coherent spin rotation of 360° from the source to drain contacts. The spin-FET studied by Schliemann, Egues, and Loss [6], however, varies the spin dephasing length from $L_{\rm SS} \ll L_{\rm D}$ to $L_{\rm SS} \gg L_{\rm D}$, by tuning the spin-orbit coupling constants.

For the device channel oriented along the (1, 0, 0) crystallographic direction ($\xi = 0$), the calculated spin scattering length for the temperatures $T = 77$–300 K at $V_{\rm DS} = 0.1$ V and $V_{\rm DS} = 0.25$ V is in the deep-submicron length scale, as shown in Fig. 3. This is consistent with the experimental results [28], where possible spin-dependent effects in a micrometer-size device disappear for $T > 190$ K. In the considered temperature range, Fig. 3 shows that the spin scattering length can be approximately described by a linear function. Effects of the inplane electric field on the spin-dephasing are considerably more pronounced at low temperatures than at high temperature.

The instant orientation of the spin-polarization vector is also one of the important characteristics of the spin-FET in addition to the spin scattering length. This property controls the selective filtering of the spin-polarized current across a semiconductor/ferromagnetic interface [29]. To provide a detailed description of the coherent evolution of the spin polarization and the spin dephasing, the magnitude and components of $\mathbf{P}(\mathbf{r})$ as a function of position in the device channel and the injected polarization should be considered. In Fig. 4, we show an example of the steady-state distribution of the spin polarization vector in the device channel at room temperature. The device channel is oriented parallel to the (1, 0, 0) crystallographic direction ($\xi = 0$). In an ideal structure proposed for the spin-FET [4], electrons propagate along the channel without scattering, and the Rashba interaction in (3) is much stronger than the Dresselhaus interaction in (4), i.e., $\eta \gg \beta \langle k_z^2 \rangle$. In this case, according to (3) the spin polarization rotates in the xz plane about the y axis. It produces coherent oscillations of the $P_x(x)$

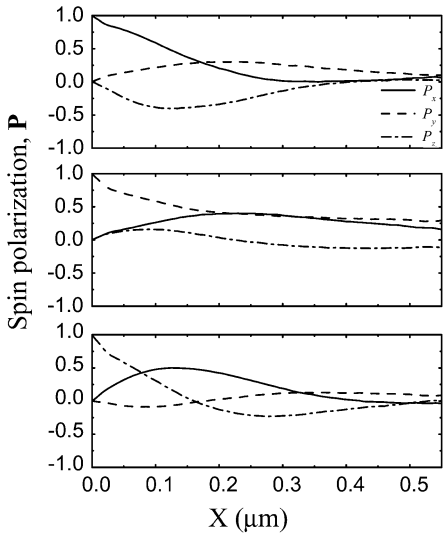

Fig. 4. Evolution of spin polarization for three different injected orientations. The device channel is parallel to the (1, 0, 0) crystallogrphic direction ($\xi = 0$). $T = 300$ K and $V_{\rm DS} = 0.1$ V.

and $P_z(x)$ components along the channel. Similar rotation of the spin polarization in the yz plane about the x axis would be observed if only the Dresselhaus spin-orbit interaction is considered. In the considered device structure, owing to the comparable strength of the Dresselhaus and Rashba spin-orbit interactions $(\eta \sim \beta\langle k_z^2\rangle)$ and electron momentum scattering, the spin polarization evolves on a spiral trajectory about an effective axis located in the xy plane. The simulated results are shown in Fig. 4. The period of the coherent spin polarization oscillation is comparable with the device length, and significantly larger than the spin scattering length, $L_{\rm D} \approx L_{360} > L_{\rm SS}$. This is contrary to the spin-FET [4] requirements. At room temperature, variations of the drain–source voltage do not produce substantial changes in $L_{\rm SS}$ (see Fig. 3). However, some improvement in this configuration $(\xi = 0)$ can be obtained using a lower temperature or finite device width [12], [13].

To analyze the instant orientation of the spin polarization vector, we introduce two spherical angles, ϕ and θ, where ϕ is measured in the xz plane, from the x axis, and θ is measured in the yz plane, from the y axis. In Fig. 5, the orientation of the polarization vector at the drain boundary for $T = 77$ K is shown as a function of the applied drain–source voltage, $V_{\rm DS}$. While the dispersion of the angle θ is relatively small, $\Delta\theta \approx 14°$, the angle ϕ varies in a range as large as 90° for $0.05\ {\rm V} < V_{\rm DS} < 0.25$ V. Both the three-dimensional (3-D) trajectory for the coherent evolution of the spin polarization and its dependence on the drain–source voltage can affect the efficiency of the spin-FET even without strong spin dephasing. While the former will complicate design by the more complex alignment of magnetization in source and drain contacts, the latter will influence the device stability.

Because the Dresselhaus interaction given in (4) is strongly dependent on the angle ξ, the spin scattering length can be effectively modulated by ξ, as illustrated in Fig. 6, where the injection spin polarization is oriented in the x direction. For $\xi = n\pi + \pi/4$, which corresponds to $(1, 1, 0)$ and $(-1, -1, 0)$

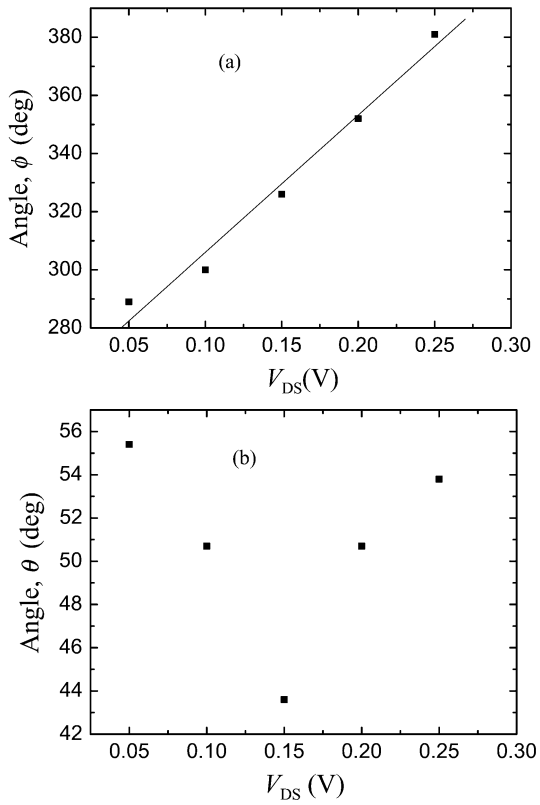

Fig. 5. Orientation of the spin polarization vector at the drain boundary at $T = 77$ K. The angle ϕ is measured in the xz plane, from the x axis, and θ is measured in the yz plane, from the y axis. ($\xi = 0$).

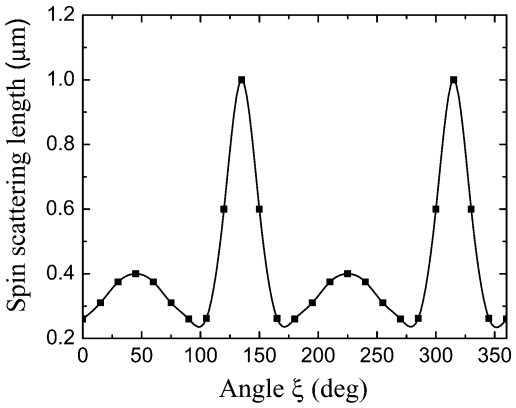

Fig. 6. Angular dependence of spin scattering length. Injected spin polarization is parallel to the device channel. $T = 300$ K and $V_{\rm DS} = 0.1$ V.

directions in the crystallographic axes, the spin dephasing is partially suppressed. The spin scattering length is maximal and exceeds the device size for the angles $\xi = n\pi - \pi/4$, corresponding to the $(1, -1, 0)$ and $(-1, 1, 0)$ directions. Its estimated value is $L_{\rm SS} = 0.9$–$1\ \mu$m. According to the simulation results in Fig. 6, the orientation of the device channel along the (1, 0, 0) or (0, 1, 0) crystallographic direction is the least appropriate choice for the spin-FET architecture. In our case, in contrast to [6], the spin dephasing is not completely suppressed for transport along $(\pm 1, \pm 1, 0)$ and $(\pm 1, \mp 1, 0)$ directions, owing to nonequal strength of the Rashba (3) and Dresselhaus (4) spin-orbit terms.

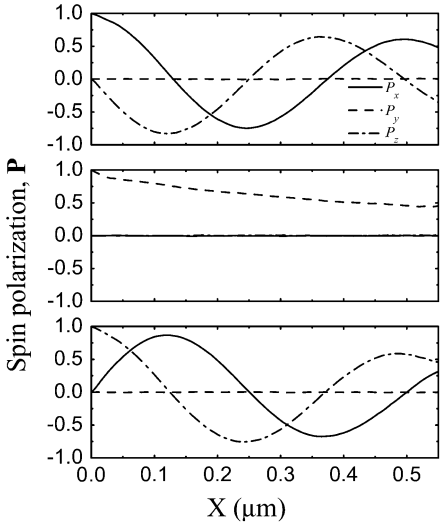

Fig. 7. Evolution of spin polarization ($\xi = -\pi/4, T = 300$ K and $V_{\rm DS} = 0.1$ V).

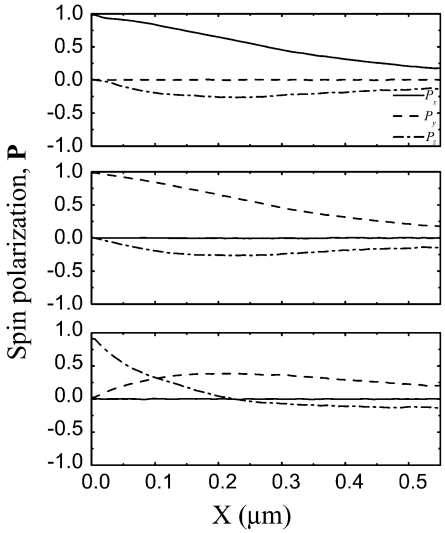

Fig. 8. Evolution of spin polarization ($\xi = \pi/4, T = 300$ K, $V_{\rm DS} = 0.1$ V).

As shown in Fig. 7, for transport along the $(\pm 1, \mp 1, 0)$ crystallographic directions, the spin dynamics is appreciably deferent in comparison with the case of $\xi = 0$ (see Fig. 4). The spin polarization vector, with the injected spin orientation parallel to the device channel (x axis), evolves in the xz plane only, as required for the ideal spin-FET [4]. The dependence of the coherent spin evolution on the inplane electric field is also suppressed in this configuration. Our simulation indicates that, at room temperature for $0.05\ \text{V} < V_{\rm DS} < 0.25$ V, the angle ϕ varies within a 20° range from 387° to 407°. The ratio between the characteristic length for the 360° coherent spin rotation and spin scattering length is $L_{360}/L_{\rm SS} \approx 1/2$.

IV. Discussion

The study has shown the importance of the considered anisotropic effect on the partial decoupling of the coherent spin oscillations and the D'yakonov–Perel spin relaxation mechanism. Proper selection of the channel direction with respect to the crystallographic axes can substantially increase the spin-dephasing length and relax the requirement of ballistic transport regime for the spin-FETs [4]. For the transport along $(\pm 1, \pm 1, 0)$ and $(\pm 1, \mp 1, 0)$ directions in the crystallographic axes, the spin scattering lengths are significantly different. In the case $\xi = n\pi - \pi/4$, the spin-orbit interaction term $H_{\rm SO} = H_{\rm R} + H_{\rm D}$ is equal to

$$H_{\rm SO} = a_{yx} k_y \sigma_x - a_{xy} k_x \sigma_y, \tag{8}$$

where

$$\begin{aligned} a_{yx} &= \eta - \beta \left\langle k_z^2 \right\rangle, \\ a_{xy} &= \eta + \beta \left\langle k_z^2 \right\rangle. \end{aligned} \tag{9}$$

If both spin-orbit coupling constants, η and β, are positive and comparable, the term proportional to σ_y in (8), responsible for the coherent evolution of the spin polarization [4], will mainly govern the spin dynamics. The injected spin polarization will evolve coherently about y axis in the device coordinate system. The term proportional to σ_x will induce spin dephasing.

If the device channel is oriented along $(\pm 1, \pm 1, 0)$ direction in the crystallographic axes (or $\xi = n\pi + \pi/4$), the spin-orbit interaction becomes

$$H_{\rm SO} = a_{xy} k_y \sigma_x - a_{yx} k_x \sigma_y. \tag{10}$$

The term proportional to σ_x will be dominant in (10). It will therefore conserve the x component of the spin polarization vector and produce spin dephasing for other components. The coherent spin evolution determined by the second term in (10) is appreciably slow in this case, as shown in Fig. 8. These results suggest that the device channel orientation along the $(\pm 1, \mp 1, 0)$ direction in the crystallographic axes is more appropriate for the spin-FET [4] design.

The issue related to the gate control of the spin dynamics is not investigated in this work. Though, in the original proposal for the spin-FET [4] and in some experimental studies of the gate control of spin-orbit coupling [28], [30], the Rashba term is assumed dominant, in the recent work [31] gate effects on the both spin-orbit interaction terms have been considered.

Though in the derived model the spatial electron transport is treated classically, it accounts for the coherent dynamics of the spin polarization. Some feedback effects of the spin-orbit interaction on the spatial transport properties [32], [33] are assumed negligible.

In comparison with other models, where the single electron spin is described as a vector [12], [13], the approach in this study using the spin density matrix description can easily accommodate the cases where electrons are not completely spin polarized, and can also incorporate spin-spin scattering mechanisms [34]. Moreover, the spin density matrix formalism can be used in the quantum mechanical description of the spin-polarized transport at low temperatures [35].

V. Conclusion

The dephasing and coherent evolution of the spin polarized current has been studied in a 550-nm length $In_{0.52}Al_{0.48}As/In_{0.53}Ga_{0.47}As$ heterostructure grown in (0, 0, 1) direction, using a Monte Carlo method developed

previously for 2-D electron spin dynamics [14]. The Rashba and Dresselhaus spin-orbit interaction terms control spin dynamics in the channel. Owing to the comparable strength of the Rashba and Dresselhaus terms, the spin dephsing and coherent spin dynamics are dependent on the channel orientation with respect to the crystallographic axes. With the channel oriented along the $(\pm 1, \mp 1, 0)$ directions in the crystallographic axes (or $\xi = -\pi/4 + n\pi$), we found that the spin-FET proposed by Datta and Das offers more desirable spin-device characteristics, and the coherent oscillations of spin polarization injected along the device channel still remain. These desirable characteristics include the maximized spin dephasing length and a smaller shift of the angle ϕ induced by the variation of the applied voltage, $V_{\rm DS}$. The spin-FET designed in this configuration will possibly operate within the nonballistic transport regime. At room temperature the estimated ratio between the characteristic length for the coherent spin rotation of 360° and spin scattering length is $L_{360}/L_{\rm SS} \approx 1/2$.

ACKNOWLEDGMENT

The authors thank Prof. V. Privman for valuable discussions.

REFERENCES

[1] S. A. Wolf, D. D. Awschalom, R. A. Buhrman, J. M. Daughton, S. von Molnar, M. L. Roukes, A. Y. Chtchelkanova, and D. M. Treger, "Spintronics: A spin-based electronics. Vision for the future," *Science*, vol. 294, pp. 1488–1495, 2001.

[2] S. D. Sarma, "Spintronics," *Amer. Sci.*, vol. 89, no. 6, pp. 516–523, 2001.

[3] D. D. Awschalom, M. E. Flatte, and N. Samarth, "Spintronics," *Sci. Amer.*, vol. 286, no. 6, pp. 66–73, 2002.

[4] S. Datta and B. Das, "Electronic analog of the electro-optic modulator," *Appl. Phys. Lett.*, vol. 56, pp. 665–667, 1990.

[5] J. Schliemann, J. C. Egues, and D. Loss, "Nonballistic spin-field-effect transistor," *Phys. Rev. Lett.*, vol. 90, no. 146 801, 2003.

[6] J. C. Egues, G. Burkard, and D. Loss, "Datta–Das transistor with enhanced spin control," *Appl. Phys. Lett.*, vol. 82, pp. 2658–2660, 2003.

[7] J. Fabian, I. Zutic, and S. D. Sarma, "Theory of spin-polarized bipolar transport in magnetic p-n junctions," *Phys. Rev. B*, vol. 66, no. 165 301, 2002.

[8] M. E. Flatte, Z. G. Yu, E. Johnson-Halperin, and D. D. Awschalom, "Theory of semiconductor magnetic bipolar transistors," *Appl. Phys. Lett.*, vol. 82, pp. 4740–4742, 2003.

[9] Magnetic bipolar transistor, J. Fabian, I. Zutic, and S. D. Sarma. [Online]. Available: http://www.arxiv.org

[10] M. I. Dyakonov and V. Y. Kachorovskii, "Spin relaxation of two-dimensional electrons in noncentrosymmertic semiconductors," *Sov. Phys. Semicond.*, vol. 20, pp. 110–112, 1986.

[11] The effect of ramsauer type transmission resonances on the conductance modulation of spin interferometers, M. Cahay and S. Bandyopadhyay. [Online]. Available: http://www.arxiv.org

[12] A. A. Kiselev and K. W. Kim, "Progressive suppression of spin relaxation in two-dimensional channels of finite width," *Phys. Rev. B*, vol. 61, pp. 13 115–13 120, 2000.

[13] A. Bournel, V. Delmouly, P. Dollfus, G. Tremblay, and P. Hesto, "Theoretical and experimental considerations on the spin field effect transistor," *Phys. E*, vol. 10, pp. 86–90, 2001.

[14] S. Saikin, M. Shen, M.-C. Cheng, and V. Privman, "Semiclassical Monte Carlo model for inplane transport of spin-polarized electrons in III-V heterostructures," *J. Appl. Phys.*, vol. 94, pp. 1769–1775, 2003.

[15] M. Shen, S. Saikin, M.-C. Cheng, and V. Privman, "Monte Carlo simulation of spin-polarized transport," in *Proc. Int. Conf. Computational Sci. Appl. (ICCSA 2003)—Lecture Notes Comput. Sci.*, vol. 2668-II, V. Kumar, M. L. Gavrilova, C. J. K. Tan, and P. L'Ecuyer, Eds., 2003, pp. 881–991.

[16] S. Pramanik, S. Bandyopadhyay, and M. Cahay, "Spin dephasing in quantum wires," *Phys. Rev. B*, vol. 68, 2003. Article 075313.

[17] K. Hess, Ed., *Monte Carlo Device Simulation: Full Band and Beyond*. ser. Kluwer Int. Series Eng. Comput. Sci., .144. Norton, MA: Kluwer, 1991.

[18] K. Tomizawa, *Numerical Simulation of Submicron Semiconductor Devices*. Boston, MA: Artech House, 1993.

[19] N. S. Averkiev, L. E. Golub, and M. Willander, "Spin relaxation anisotropy in two-dimensional semiconductor systems," *J. Phys. Condens. Matter*, vol. 14, pp. R271–R283, 2002.

[20] K. Blum, *Density Matrix Theory and Applications*. New York: Plenum, 1996.

[21] U. Haeberlen, *High Resolution NMR in Solids (Advances in Magnetic Resonance Series, Supplement 1)*. New York: Academic, June 1976.

[22] G. Dresselhaus, "Spin-orbit coupling effects in zinc blende structures," *Phys. Rev.*, vol. 100, pp. 580–586, 1955.

[23] Y. Bychkov and E. I. Rashba, "Oscillatory effects and the magnetic susceptibility of carriers in inversion layers," *J. Phys. C*, vol. 17, pp. 6039–6045, 1984.

[24] E. A. de Andrada e Silva, G. C. La Rocca, and F. Bassani, "Spin-split subbands and magneto-oscillations in III-V asymmetric heterostructures," *Phys. Rev. B*, vol. 50, pp. 8523–8533, 1994.

[25] M. Cardona, N. E. Christensen, and G. Fasol, "Relativistic band structure and spin-orbit splitting of zinc-blende-type semiconductors," *Phys. Rev. B*, vol. 38, pp. 1806–1827, 1988.

[26] V. Fischetti and S. E. Laux, "DAMOCLES Manual," IBM, Apr. 1995.

[27] A. Tackeuchi, O. Wada, and Y. Nishikawa, "Electron spin relaxation in InGaAs/InP multiple-quantum wells," *Appl. Phys. Lett.*, vol. 70, pp. 1131–1133, 1997.

[28] Y. Sato, S. Gozu, T. Kita, and S. Yamada, "Study for realization of spin-polarized field effect transistor in $In_{0.75}Ga_{0.25}As/In_{0.75}Al_{0.25}As$ heterostructure," *Phys. E*, vol. 12, pp. 399–402, 2002.

[29] A. Hirohata, S. J. Steinmueller, W. S. Cho, Y. B. Xu, C. M. Guertler, G. Wastlbauer, J. A. C. Bland, and S. N. Holmes, "Ballistic spin filtering across ferromagnet/semiconductor interfaces at room temperature," *Phys. Rev. B*, vol. 66, no. 035 330, 2002.

[30] J. Nitta, T. Akazaki, and H. Takayanagi, "Gate control of spin-orbit interaction in an inverted $In_{0.53}Ga_{0.47}As/In_{0.52}Al_{0.48}As$ heterostructure," *Phys. Rev. Lett.*, vol. 78, pp. 1335–1338, Feb. 1997.

[31] J. B. Miller, D. M. Zumbuhl, C. M. Marcus, Y. B. Lyanda-Geller, D. Goldhaber-Gordon, K. Campman, and A. C. Gossard, "Gate-controlled spin-orbit quantum interference effects in lateral transport," *Phys. Rev. Lett.*, vol. 90, no. 076 807, 2003.

[32] J. Inoue, G. E. W. Bauer, and L. W. Molenkamp, "Diffusive transport and spin accumulation in a Rashba two-dimesional electron gas," *Phys. Rev. B*, vol. 67, no. 033 104, 2003.

[33] J. Schliemann and D. Loss, "Anisotropic transport in the two-dimensional electron gas in the presence of spin-orbit coupling," *Phys. Rev. B*, vol. 68, no. 165 311, 2003.

[34] Y. V. Pershin and V. Privman, "Spin relaxation of conduction electrons in semiconductors due to interaction with nuclear spins," *NanoLett.*, vol. 3, pp. 695–700, 2003.

[35] Entanglement of electron spin and orbital states in spintronic quatum transport, B. K. Nikolic. [Online]. Available: http://www.arxiv.org

Semion Saikin was born in Kazan, Russia. He received the M.S. degree in physics and the Ph.D. degree in theoretical physics from the Kazan State University, Russia, in 1995 and 1998, respectively.

Since 1999, he has been an Assistant Professor at the Theoretical Physics Department, Kazan State University. On leave of absence from Kazan State University since 2001, he has been a Postdoctoral Research Associate at the Center for Quantum Device Technology, affiliated with the Department of Electrical and Computer Engineering, Clarkson University, Potsdam, NY. His research interests center on the field of solid-state physics with an emphasis on application to modern device technology, including microscopic structure of crystals and evolution of open quantum systems for quantum computation and spintronics application.

Min Shen was born in Shanghai, China. He received his B.S. degree in electrical engineering and M.S. degree in fluid mechanics from Shanghai University of Technology (now Shanghai University), China in 1982 and 1987, respectively.

From 1982 to 1984, he was a Lecturer at the Shanghai Polytechnic School of Electronic Instruments. From 1987 to 1998, he was with the Institute of Applied Mathematics and Mechanics at Shanghai University. From 1998 to 1999, he was a visiting scholar in the Advanced Material Research Institute at University of New Orleans, New Orleans, LA. From 2000 to 2001, he was with Celestica International Inc., Toronto, Canada. He joined Clarkson University, Potsdam, NY, as a Research Assistant in 2002, where he is currently working toward his Ph.D. degree in electrical engineering. His research interests include modeling and simulation of nanoscale electronic and spintronic devices, transient heat flow models of SOI devices, heat and mass transfer in engineering processes and computational fluid dynamics.

Mr. Shen coauthored the paper that received the Best Paper Award from the 2003 IEEE Conference on Electron Devices and Solid-State Circuits (EDSSC).

Ming-C. Cheng (M'90) was born in Kaohsiung, Taiwan. He received the B.S. degree in electrophysics from the National Chiao-Tung University, Taiwan, in 1980, and the M.S. degree in system engineering and the Ph.D. degree in electrical engineering from the Polytechnic University, New York, in 1986 and 1990, respectively.

From 1982 to 1984, he was as an Electronic Engineer at ITT in Taiwan. He was with Department of Electrical Engineering, University of New Orleans from 1990 to 2000. Since 2000, he has been an Associate Professor in Department of Electrical and Computer Engineering, Clarkson University, Potsdam, NY. He has been involved in transport models for advanced semiconductor devices, optimization of microelectronic devices and heat flow models for SOI devices and interconnects. His current research interests are in general concerned with simulation and physical modeling of next-generation solid-state devices, including quantum spintronic devices and compact modeling of heat flow in SOI structures.

Dr. Cheng received the Best Paper Award from the 2003 IEEE Conference on Electron Devices and Solid-State Circuits (EDSSC). He is also the recipient of the NSF Research Initiation Award in 1995 from the Solid State and Microstructures Engineering Program.